

Appendix B

DSC, TMDSC AND LISSAJOUS FIGURES

Lissajous Figures for Understanding Temperature Modulated Differential Scanning Calorimetry of Nylons

This appendix covers some work that is associated with the thesis and is worth recording but does not fit so neatly in the main thrust of the work

B.1 Introduction

Differential Scanning Calorimetry (DSC) has been a valuable tool for investigating the melting, crystallisation and recrystallisation characteristics of polymers.

Standard DSC instruments can be of two types “Power Compensated”-and “Heat Flux”.

“Power Compensated” instruments maintain the reference and the sample pans at the same temperature during the applied heating cycle. Separate heaters in the DSC cell for each pan maintain a zero temperature difference between sample and reference pans. The power supplied to each pan is monitored so the difference in the applied power can be used to calculate the heat flow.

“Heat Flux” instruments use an alternative method where both pans are heated from a single heating source in the DSC cell walls. The temperature difference between the two pans is monitored using thermocouples positioned under the sample and reference pans. The actual heat flow into or out of the sample pan is calculated from the measured temperature difference. This approach is that used by TA Instruments equipment in this work.

A Heat Flux instrument, model 2920 supplied by TA Instruments and equipped with a standard cell, was used for this work. This cell is constructed using heating elements wound around a vertical silver cylinder. A thin constantan disk is fitted horizontally across the middle of the DSC cell. The constantan disk supports the sample and reference pans on raised

dimples equidistant from the heating block. Two fine wires welded underneath the sample and reference pan dimples to chromel disks immediately below, form area thermocouples with the constantan. These are connected back-to-back so that the difference in temperature between the sample and reference is directly measured. The construction geometry of the cell is such that the thermal resistance from the heating block to the both pans is the same.

Newton's Law of Heat Flow is used to calculate the heat flow in and out of the sample Newton's Law, between two locations 1 and 2 of differing temperature, is essentially given by Equation B-1.

$$\frac{dQ_{12}}{dt} = \lambda \times \Delta T_{12} \quad \text{Eqn. (B-1)}$$

where dQ_{12}/dt is the overall rate of heat flow, t is time, λ is the thermal conductivity of the path between the two locations and ΔT_{12} is the difference in temperature between the two locations.

Essentially this specifies that the heat flows from the heating block (nominally through the constantan disk) to the dimples are proportional to the temperature differences between the heating block temperature (T_b) and either of the dimples. The cell relies on the thermal resistance between walls and the reference or sample dimples in the constantan disk being the identical. Newton's constant (λ) is thus the same in each case and is effectively incorporated into the experimentally determined Cell Constant K .

Thus:

$$\frac{dQ_{br}}{dt} = \lambda \times (T_b - T_r) \quad \text{Eqn. (B-2)}$$

and

$$\frac{dQ_{bs}}{dt} = \lambda \times (T_b - T_s) \quad \text{Eqn. (B-3)}$$

Subtracting Equation B-2 from Equation B-3 effectively eliminates the block temperature (T_b) and provides the heat flow difference, dQ_{sr}/dt , between the sample and reference dimples. This simplification demonstrates that the difference in heat flow between the sample and reference (dQ_{rs}/dt) from or to the block can be determined as shown in Equation B-4.

$$\frac{dQ_{rs}}{dt} = \lambda \times (T_r - T_s) \quad \text{Eqn. (B-4)}$$

Back-to-back thermocouples are used to directly measure the heat flow into the sample relative to that into the reference utilising the constant of proportionality from block-to-dimple thermal resistance.

The cell is used with a purge gas flow into the lower and upper halves of the cell ensuring a quick response to changes in heat flow. Two gasses that are commonly used are nitrogen and helium. Helium has greater heat conductivity than nitrogen, thereby transporting heat to and from the cell walls, the constantan disk and the samples more efficiently than nitrogen. Nitrogen is commonly used in preference to helium however due to its much lower cost.

The idealised DSC cell assumes all heat to and from the reference and sample occurs via the thermally conductive constantan disk. Wunderlich [161] has also argued that the lower thermal conductivity of nitrogen gas (compared to helium gas) ensures the DSC operates more ideally, whereby heat transfer occurs more readily through the constantan disk and less readily via the gas.

However, in reality, the constantan disk and gas operate in parallel to form the thermal paths.

In general, the heat flow into or out of a sample of material is made up of thermodynamic effects and kinetic effects. The thermodynamic component is dependent only upon the heat capacity of the material and the rate of change of temperature. The kinetic effects will be dependent on a function of the temperature and time history of the sample material.

This is written [129] for a sample in Equation B-5 as:

$$\frac{dQ_s}{dt} = -C_p \times \frac{dT_s}{dt} + f[T, t] \quad \text{Eqn. (B-5)}$$

where C_p is the Heat Capacity function at constant pressure and $f(T, t)$ is a function of temperature and time. It is important to appreciate that in DSC and TMDSC that C_p is not constant but is variable with respect to temperature.

It can be seen that the heat capacity can be determined by deliberately changing the heating rate and examining the way that heat flow changes. Thermodynamic changes can be classified as reversible within the context of

an experiment, provided that thermal processes occur at a rate that is significantly faster than the heating rate changes. Examples of thermal properties that are generally considered to be reversible are glass transitions and heat capacity.

On the other hand, the kinetic component, dependant on temperature and time, is independent of the heating rate. Examples of these are non-reversible processes such as decomposition, evaporation, curing reactions, and changes from metastable crystalline structures to more stable ones.

Sometimes there are events that appear to have both reversible and non-reversible characteristics. It has been postulated that thermodynamically reversible events may occur on a time frame that is similar to or slower than the speed of variation in heating rate. A transition will seem in such situations to have a mixed reversible/non-reversible character [134] or in some instances may appear completely non-reversible. An example of this is the melting of polymer crystals. There have been careful experiments by Okazaki and Wunderlich [40] showing that melting of poly(ethylene terephthalate) PET can be completely reversible over small temperature ranges where macromolecular chains partly melt from polymer crystals. A fully molten macromolecule would require (non-reversible) re-nucleation due to a free-enthalpy barrier to the crystallisation. Glass transitions can also display some non-reversible character [133, 162] when evaluated by TMDSC. Standard DSC merely measures the total heat flow rather than separating out the components.

Heat Capacity (C_p) can be determined by measuring different samples at different heating rates in conventional DSC. The original thermal history would be destroyed in the first run if the same sample were to be run twice. Use of two samples also means a loss in accuracy because of the potential for weight measurement errors. The time taken to carry out the experimental runs is also longer, reducing throughput.

Another problem with DSC is a requirement for small samples to achieve good resolution, which conflicts with the requirement for larger samples to achieve higher sensitivity. The temperature differential within (normally) poorly conducting polymer samples is greater if the sample is larger. This leads to a spreading of sharp transitions due to different parts of the sample

being at slightly different stages of the heating ramp, and thus a loss in resolution.

1993 saw the advent of Temperature Modulated Differential Scanning Calorimetry (TMDSC) [131, 163-166]. TMDSC superimposes a modulated heating rate on top of a constant heating ramp normally used in most DSC experiments. Most equipment manufacturers for TMDSC use sinusoidal modulation, but sawtooth modulation has also been employed. The period of the modulations is generally limited by physical factors and occurs in a range 10 to 100 s for commercially available equipment. The discussion here considers only the mathematical and graphical ramifications of sinusoidal modulations.

Two further parameters are necessary to define the experimental system; the amplitude A_s ($^{\circ}\text{C}$) of the sinusoidal temperature modulation at the sample; and P (sec), the period of the modulation [129].

Temperature (T_s) of the sample at a particular time (t) once the system has achieved steady state is given [40] by Equation B-6:

$$T_s = T_0 + \langle q \rangle \times t - \langle q \rangle \times \frac{C_s}{\lambda} + A_s \times \sin(\omega \times t - \varepsilon) \quad \text{Eqn. (B-6)}$$

The corresponding linear temperature expression for conventional DSC in steady state is given by Equation B-7:

$$T_s = T_0 + \langle q \rangle \times t - \langle q \rangle \times C_s \quad \text{Eqn. (B-7)}$$

where:

T_s is the sample temperature at time t .

T_0 is the starting temperature of the heating block, the reference pan and the sample pan with its sample,

$\langle q \rangle$ is the average or underlying heating rate,

t is the time (s).

ω is the modulation frequency (s^{-1}) and equals $2\pi/P$.

ε is the phase lag in radians between the block and the sample pan.

λ is the thermal conductivity of block-pan path as mentioned previously.

and C_s is the heat capacity of the sample pan (including any sample). The term with C_s is caused by the temperature lag of the sample behind the temperature applied to the block. There is an exponential lead-in to the steady state condition at the start of the experiment and tends to zero as steady state is approached.

There are virtually identical equations for T_r , the reference temperature with subscripts r instead of s and a phase lag of ϕ for the empty reference pan that is different from ε for the matched sample pan with sample.

The sinusoidally modulated heat flow into and out the sample pan, due to the heat capacity of the sample itself, is still determined by Equation 4 and is proportional to the instantaneous difference in sample and reference temperatures. It will have a sinusoidally changing amplitude with a phase difference δ between block and ΔT .

There will then be a measurable phase lag of Φ between the measured sample temperature T_s and the measured heat flow given by the difference between ε and δ .

This difference Φ in phase between the sample temperature and the heat flow will become more apparent in the discussion of Lissajous figures and is shown in the figures presented later in this paper.

A common procedure in TMDSC experiments is to apply a modulation amplitude such that, whilst heating, the temperature rate never goes negative, or during cooling, never goes positive. For example, an amplitude of 0.212 °C results in heating rates varying from zero to close to 4 °C/min at an average heating rate of 2 °C/min and period of 40 s.

The advantages of such an experimental method are numerous.

1. Both sensitivity and resolution are increased. The portions of a modulated heating ramp with a high heating rate contribute a large signal, increasing sensitivity. The reason for this can easily be seen from Equation B-4 in that the heat flow signal will increase markedly as the heating rate increases.

At the same time, the overall heating rate is slower than if the sample had been ramped continuously at the maximum rate for the whole time. The

slower average heating rate with TMDSC overcomes the problem that would have been encountered with temperature gradients and thermal lags [134].

This means that samples as low as 2 or 3 mg may still be used in combination with the high and low heating rates of TMDSC to achieve a good signal. This compares with the 10 to 20 mg usually used in standard DSC. Commonly sample sizes of 5 to 10 mg are used with TMDSC and these are preferable, in the case of polymers to samples of 20 mg because of the delays inherent in heat transfer from the outside to inside of a sample. The small sample size is necessary because of the generally poor heat conductivity of polymers (*vide supra*). One of the conditions of accurate TMDSC work is that there is minimal temperature variation within the sample.

2. The sample never goes into cooling during heating with a modulation procedure of this nature. Whilst this is less important for the analysis of rapid thermodynamic transitions such as glass transitions that are experimentally reversible. This is not the case for slower reversible transitions, such as polymer melting. It is possible during melting that unwanted recrystallisation may occur during a short cooling phase of the modulation and that is not considered to be beneficial. No such cooling phase occurs using the heating profile described above.

3. The experimental setup for the described modulation is such that the heating rate is actually 0 °C/min at the slowest part of the heating cycle. We can see from Equation B-5 that at this point $dT/dt=0$. Therefore all heat flow is non-reversible, that is $dQ/dt= f(T,t)$. It is possible to use this feature of TMDSC to check that the cell constant and heat capacity constant are correct by the alignment of the modulated heat flow at $dT/dt=0$ with the derived continuous non-reversible heat flow.

Another criterion is that the response is linear [132, 133, 167, 168]. Linearity occurs where doubling the temperature modulation amplitude leads to a measured doubling of the heat flow response. That is generally not the case during major transitions where materials are rapidly changing from one phase or morphology into another [169].

Equation B-5 clearly demonstrates that reversible heat flow is a function of heating rate and sample heat capacity. There is an enormously large and rapid increase in heat capacity during melting. This, combined with the

modulated heating rate that also varies, results in an extraordinary variation in thermal conductivity of a polymer sample during melting. As a result, it would appear that accurate measurement of heat capacity, and hence reversing heat flow, is unlikely during melting of a sample. A restriction on the applicability of TMDSC is that the heat capacity of the material should not change significantly during a modulation cycle [132, 133]. This also calls into question the applicability of TMDSC to melting (or crystallisation).

Accurate TMDSSC measurements require a DSC cell that responds quickly and precisely with the modulated temperature signal to rapid heating and cooling rates. It is also necessary to have a quick response between the thermal driving force (electric heating elements) or cooling system and the sample & reference pans.

Multiple thermal paths between the walls of the cell and the pans and between the two pans can influence TMDSC measurements. The primary heat transfer path is generally considered to be via the constantan disk and another path is via the gas flowing in the cell. Most authors [129, 170, 171] have chosen to ignore or play down the role of the gas in thermal transport. These two paths have different speeds of transferring heat to or from the walls, and possibly between thermocouple and sample. This may influence TMDSC measurements that are a dynamic situation with varying heating rates as distinct from the more equilibrium situation of conventional DSC with constant heating rates.

Newton's constant λ is not easily measured for each of the heat transfer paths on their own (eg. constantan disk and purge gas). Therefore a cell constant is determined which effectively incorporates Newton's for all heat transfer media together.

Only one set of calibration and cell constants is possible with the currently available software. Different calibration and cell constants are necessary for different experimental conditions. It means that if the heating ramp is run under one set of conditions eg a ramp rate of 2 °C/min and cooling is under other conditions eg. 0.5 °C/min then only the one part is able to properly run under calibrated conditions. As a result, instrument makers are continuously striving to improve cell design providing greater flexibility.

The measured heat capacity is found in TMDSC with its varying heating rates by comparing the amplitudes of the driving modulated heating rate and the resulting heat flow. The Reversing component can be isolated from the total by considering only the amplitudes of the swings in heat flow and heating rate [133, 170]. This is achieved by taking a discrete Fourier transform of the data at the modulation frequency.

$$C_p = K_{C_p} \times \frac{\text{Modulated Heat Flow amplitude}}{\text{Modulated Heating Rate amplitude}} \quad \text{Eqn. (B-8)}$$

where K_{C_p} is an instrument heat capacity calibration constant for the particular experimental conditions.

The derivative of Equation B-6 with respect to time (dT_s/dt) is given by Equation (B-9) and describes the modulated temperature (heating) rate of the sample.

$$\frac{dT_s}{dt} = q - \omega A_s \cos(\omega t - \varepsilon) \quad \text{Eqn. (B-9)}$$

From Equation B-6, the amplitude of the modulated sample temperature is given by A_s and we can see from Equation B-9 that the amplitude of the sample temperature (heating) rate is given by ωA_s . This results in a phase change difference between the modulated sample temperature (T_s) and the modulated heating rate of the sample (dT_s/dt) of $\Pi/2$. The difference has ramifications discussed in the Lissajous section below. The use of the derivative of heating rate has advantages for non-isothermal work in that it removes the effects of the sample temperature creeping upwards at the average rate of the underlying heating rate $\langle q \rangle$.

There is another form of the relationship as seen in Equation B-10 that occurs regularly [129 p. C-17, 170, 172] with quasi-isothermal work where the average heating rate is zero. There, the denominator is the amplitude of the temperature swings as a result of some simplifications for this special case.

$$C_p = K_{C_p} \times \frac{\text{Maximum Heat Flow amplitude}}{\text{Maximum Temperature amplitude} \times \omega} \quad \text{Eqn. (B-10)}$$

TMDSC measures the Total Heat Flow (from the average over a cycle). The heat capacity C_p can continuously be determined using Equation (B-8). The heat capacity must be accurately calibrated in order to calculate the correct “Reversing” Heat Flow. The “Non-reversing” heat flow will also be wrong if this is incorrectly determined because it is found in Equation (B-11) by the difference between the Total Heat Flow and the Reversing Heat Flow from Equation (B-9).

$$\text{Non - Reversing Heat Flow} = \text{Total Heat Flow} - \text{Reversing Heat Flow} \quad \text{Eqn. (B-11)}$$

The Total Heat Flow is the experimentally determined heat flow from the average over a cycle and the Reversing Heat Flow is obtained from the modulated heat flow signal after the equipment has been calibrated under identical conditions using the heat capacity of a known material.

It is necessary to firstly measure the C_p of a material with well-characterised C_p (eg sapphire/ Al_2O_3). The experimentally determined heat capacity constant K_{C_p} is essentially a second multiplier constant determined under modulating conditions of testing which becomes a multiplier of the experimentally determined cell constant (which itself is a multiplier to the experimentally determined heat flow). This must be done under the same conditions of purge gas type and flow, average ramp rate, period and amplitude that are to be used for the experimental work.

The Heat Capacity (C_p) calibration is an extremely important part of obtaining correct Reversing Heat Flow and Non-Reversing Heat Flow results from the TMDSC approach. The determination of the correct Reversing Heat Flow signal is important because the Non-Reversing result is obtained by subtracting the Reversing signal from the Total Heat Flow signal. That Total Heat flow is obtained by taking the average heat flow signal over one cycle. Sapphire (Al_2O_3) is a material with heat capacity well known in the literature from various thermal measurements. It has the advantage that it has no thermal transitions from sub-zero temperatures to well over the 600 °C maximum working temperature of the instrument. The values of C_p for the material increase monotonically from 0.718 at 0 °C to 1.000 at 180 °C and 1.0895 at 300 °C.

The K_{C_p} to achieve the correct C_p value varies with temperature. The results over a range of interest are averaged to give the best overall result. This will

obviously mean that inaccuracies in C_p measurement at temperatures other than the middle of the range can creep in. For example, the K_{Cp} required in one calibration run for 167 °C was 0.6897 and at 247 °C it was 0.7214, a 4.5% change over 80 °C. An 80 °C temperature range of melting temperatures in a single experiment can be quite normal and it cannot always be predicted beforehand what the exact range of interest will be. This means that the Reversing signal is under or over-estimated, and thereby the Non-Reversing signal is over-or under-estimated to an equivalent amount. The nature of the TA Instrument 2920 DSC software is that it is virtually impossible to adjust the results afterwards once the single K_{Cp} has been entered before the experimental run. That is, unless the data is exported to an ASCII datafile, imported into a spreadsheet such as Excel and the data manipulated further.

An error in the calibration of heat capacity in TMDSC experiments will be clearly reflected in the measurements of both the reversing and non-reversing heat flows. It is an indicator for possible incorrect C_p calibration when exact “mirroring” of Reversing and Non-reversing components [171] is seen. Incorrect C_p calibration leads to the Reversing and Non-reversing components being “measured” inaccurately. That is why heat capacity calibration is so important.

The correct allocation of reversing and non-reversing heat flows allows the separation of the thermodynamic and kinetic components of the material.

Scherrenberg [172] raises the point that if the time scale of reversible processes in the polymer differ too much from the period of the measurement, they will not be “seen” by the experiment. This is also alluded to in Simon & McKenna’s paper [170] and Xu, Li and Feng’s work [171].

B.1.1 Lissajous Figures

A Lissajous Figure is generated when one sinusoidal curve is plotted on the y-axis against another sinusoidal curve on the x-axis. This will result in a closed ellipse if the frequencies of the two curves are the same. There will be a straight line produced if the two curves are in phase. An ellipse will be produced when there is a phase lag between the two sinusoidal curves. Plotting the heat flow in a TMDSC experiment against the time derivative of sample temperature (or against the temperature for a quasi-isothermal

experiment) will create a Lissajous Figure. These can be seen in the work of several authors [40, 171, 173-179].

The slope of the straight line in the very ideal case of zero phase difference will be proportional to the heat capacity of the sample when matched pans are used for reference and sample. This is depicted in Figure B-1 for two differing heat capacities and in-phase sinusoidal curves in the use of TMDSC.

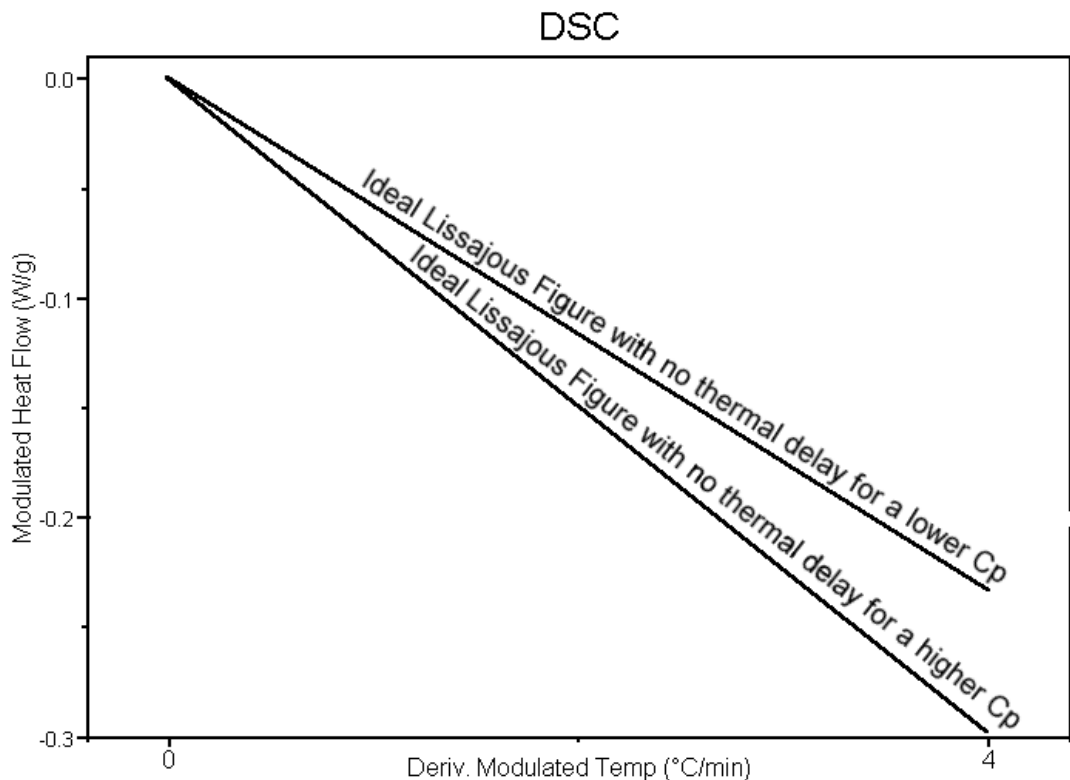


Figure B-1 Representation of Lissajous figures at two heat capacities in the ideal case with zero phase lag in the cell between sample and reference.

There are a number of causes for phase lags to occur. Phase lag occurs because there is a time difference between the modulated temperature signal measured at the reference and the sample thermocouples. This time lag may be instrumental. Factors such as:

- a) Reference and sample thermocouple not symmetrically positioned.
- b) Variation in the constantan disk creating uneven heat flow to the sample and reference thermocouples.
- c) Chromel disks and thermocouples for the reference and sample may not be identical resulting in heat flow variations.
- d) Non-uniform heating block.

- e) Uneven heat flow via the purge gas.
- f) Unequal thermal resistance between the constantan dimples and the two calorimeter pans.

In addition to this, thermal conductivity of samples can vary during thermal transitions (such as melting) due to associated large variations in sample heat capacity. Rapid, large thermal conductivity variations by a sample can induce short-term phase lags between the sample and reference pans.

Zero phase lag would be ideal for TMDSC analysis, or failing this, possibly a constant phase lag. However, in reality this is not the case.

An ellipse will be generated for TMDSC when the modulated heat flow is out of phase with the sample temperature derivative and a phase lag Φ has developed between the signals.

Drift of the Lissajous figure can occur if:

- a) the kinetic component of heat flow $f(T,t)$ is changing,
- b) the heat capacity is changing, in particular during transitions, or
- c) dT_s/dt is varying, for example during transitions.

Distortions arise if the heat flow process is nonlinear.

B.2 Experimental

B.2.1 The Choice of TMDSC Experimental Conditions For Trials

The choice of experimental conditions for DSC work is important, but this is much more the case for TMDSC work. Constraints on experimental conditions can sometimes be conflicting:

- a) The period should be as long as possible but at the same time should give 3 to 4 cycles during transitions.
- b) The instrument should retain accurate control of heating and cooling the pans in order to provide repeatable results. A maximum cooling rate of 25 °C/min used during cooling to maintain instrumental control with the TA Instruments 2920 operating in the range 300 °C down to 25 °C and the LNCA setting on switch position 3.
- c) Non-isothermal modulation should not have an amplitude great enough to give negative heating rates during ramping through melt transitions,

otherwise unwanted re-crystallisation can occur during the cooling phase, unduly influencing the results.

- d) The empty reference pan should match the sample pan (and lid) to within 100 μg [129].

The method chosen to comply with the last point above was to select a series of hermetic pans and lid combinations that were spaced apart in mass by not more than 200 μg for use as reference pans after crimping. Pans and lids used for samples could then easily be paired with an appropriate reference pan that was within the 100 μg variation limits. Lids were usually chosen to provide pairings that were much better than the above limits. An ATI Cahn C-34 balance capable of weighing to 3 to 5 μg was used.

Many of the transitions experienced with sample materials used in general with research work had sharp transitions and there is a requirement from the Fourier transformation process that at least four cycles should occur over a transition to avoid artefacts [148]. Therefore the cycle period used in this experimental work was 40 s. Helium purge gas was used for polyamide-4,6 with the cycle periods of 40 s, better than the instrument manufacturer's recommendations [129] for use with 30 s or less, and in the light of the findings here on Lissajous Figures.

The appropriate amplitude for a heating ramp rate of 2 $^{\circ}\text{C}/\text{min}$ with a 40 s period was 0.212 $^{\circ}\text{C}$ in order to maintain a zero or positive heating rate during the whole ramp [148].

B.2.2 Experimental Runs

Baseline calibrations over the range 25-320 $^{\circ}\text{C}$ were run with an empty cell. Cell Constant & Temperature calibrations were carried out with indium over the range 140-170 $^{\circ}\text{C}$ at a ramp rate of 2 $^{\circ}\text{C}/\text{min}$ for work with either helium or nitrogen purge gas flow in both parts of the cell. The indium calibrant was pre-melted and solidified in the pan to give good thermal contact.

The Heat Capacity constant K_{Cp} was calibrated with Al_2O_3 at 2 $^{\circ}\text{C}/\text{min}$ in the range 170-230 $^{\circ}\text{C}$ and/or 260-310 $^{\circ}\text{C}$, using a modulation amplitude of 0.212 $^{\circ}\text{C}$ and 40 s period.

All calibrations were carried out using identical helium or nitrogen gas flow and average ramp rate to be used in the final experiments.

TMDSC Measurements were carried out for polyamide-4,6 in the range 25-315 °C at 2 °C/min using helium purge gas at 50 ml/min. Polyamide-4,6 melts at approximately 290 °C.

B.3 Results and Discussion

The Lissajous plot in Figure B-2 shows that, under modulated conditions, a number of 40 s loops taking several minutes to stabilise, are required to achieve stabilisation. There is a feedback loop so that the block temperature modulations are modified dynamically to give the required modulation amplitude of the sample temperature. A major transition, such as melting, must be expected to take some time to restabilise the modulations.

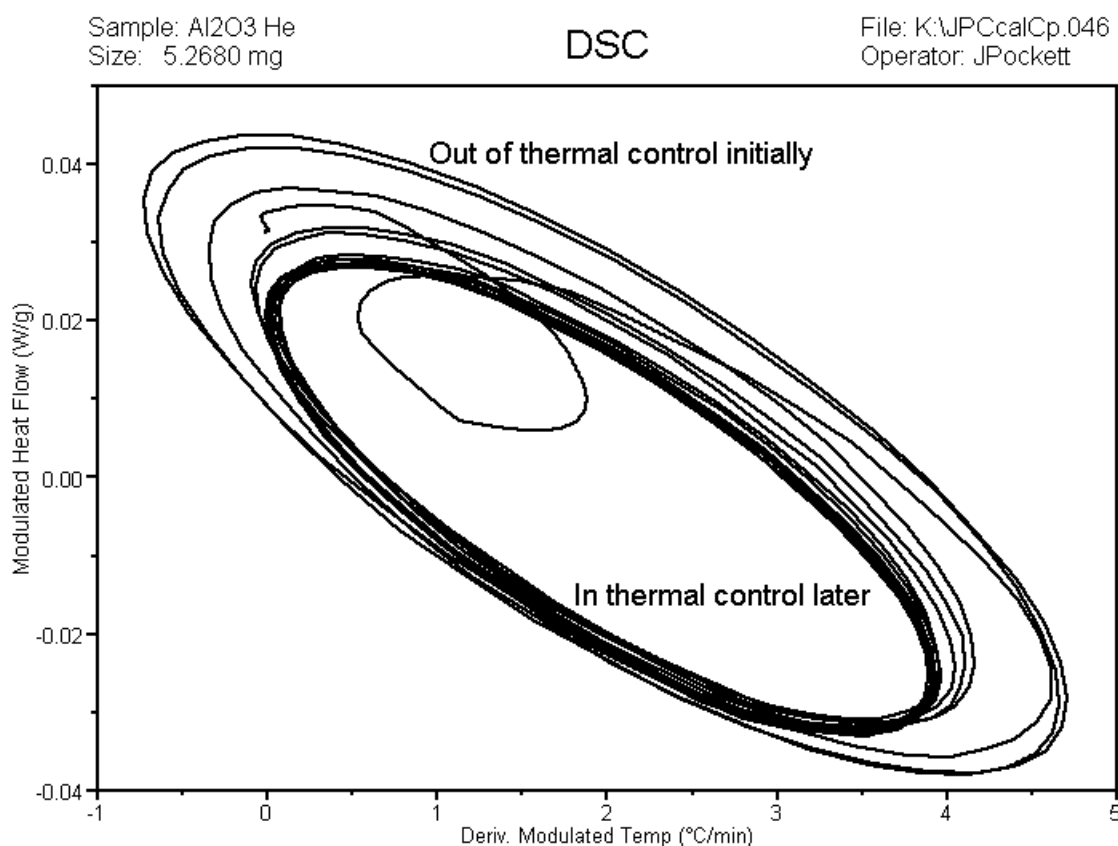


Figure B-2 Lissajous Figure of an Al₂O₃ sample achieving thermal control at the start of a TMDSC experiment. Average heating rate is 2 °C/min with a period of 40 s, an amplitude of 0.212 °C and 50 ml/min helium purge gas.

The comparison between Figure B-3 and Figure B-4 is instructive because it displays the difference in Lissajous figures of Al₂O₃ in changing from helium to nitrogen purge gas at the same flow rate and with all other instrumental conditions being identical. Only one loop is displayed in each figure in order to demonstrate the delays clearly but the loops are very typical of those found experimentally. It is clear from Figure B-3 and Figure B-4 that the ellipse from the nitrogen gas is pointing at approximately 90° to that

Sample: Al₂O₃ N₂
Size: 5.2680 mg

DSC

File: JPCcalCp.035
Operator: JPockett

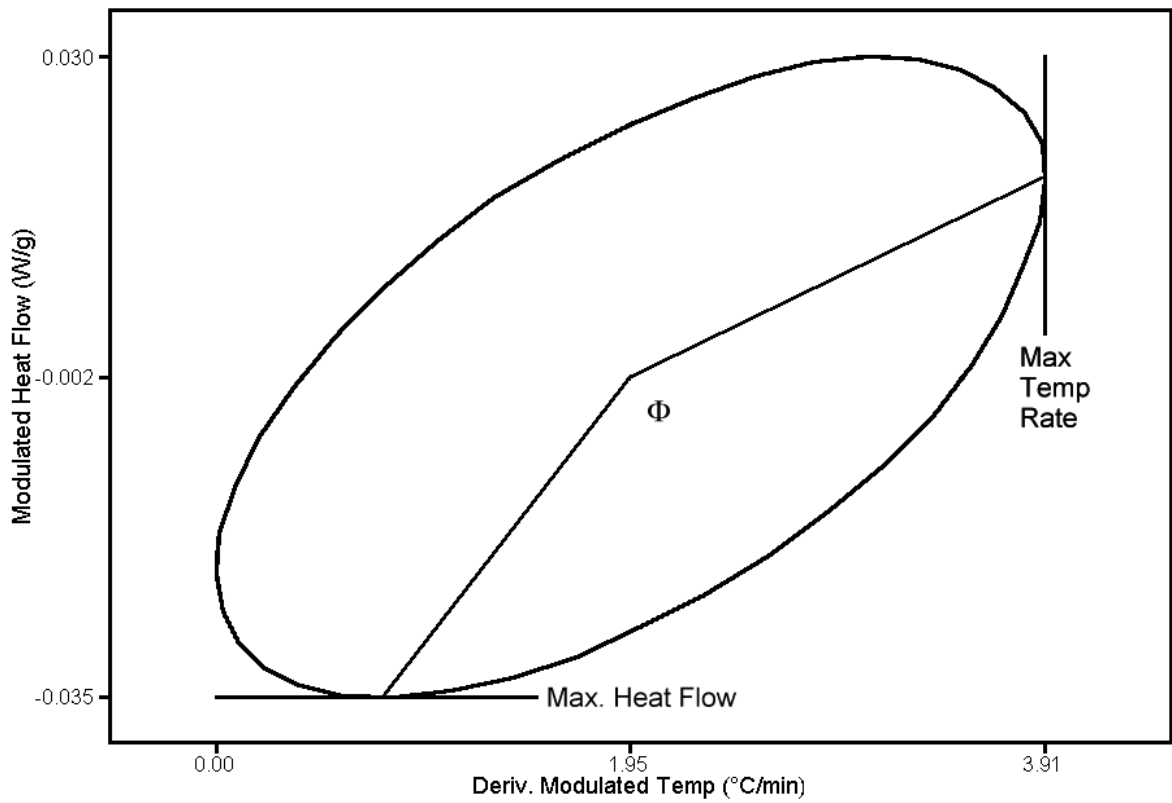


Figure B-4 Lissajous Figure for Al₂O₃ sample displaying the phase lag Φ with TMDSC for a 50 ml/min nitrogen purge gas flow, heating rate of 2 °C/min, period of 40 s and an amplitude of 0.212 °C.

Sample: Al₂O₃ 25ml/min He flow
Size: 5.2680 mg

DSC

File: K:\JPCcalCp.033
Operator: JPockett

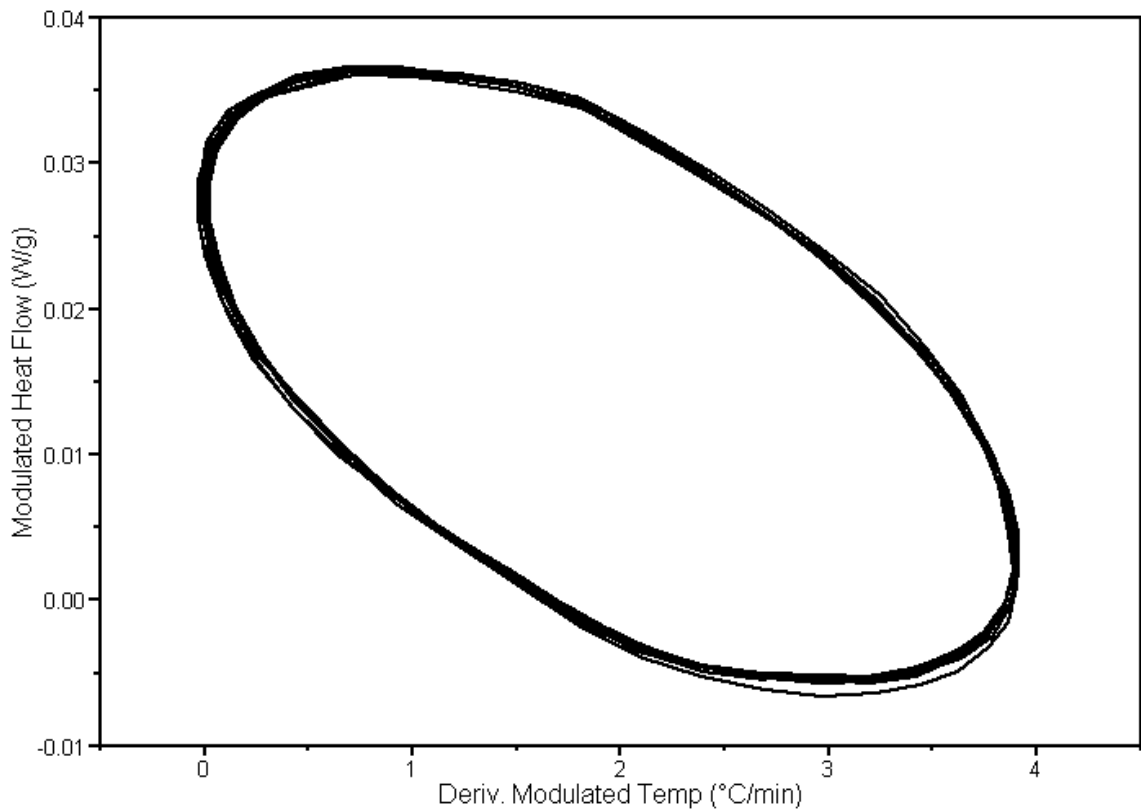


Figure B-5 Lissajous Figure for Al₂O₃ sample with TMDSC for a 25 ml/min nitrogen purge gas flow, heating rate of 2 °C/min, period of 40 s and an amplitude of 0.212 °C.

The Lissajous ellipse for helium becomes rounder when the gas flow is reduced substantially. That is also demonstrated by Cser's work [148] where he shows that even at 50 ml/min there is starting to be a change from the results at 75 and 100 ml/min. This can be seen in Figure B-5 where the helium flow was set at 25 ml/min in both purge gas streams rather than 50 ml/min. In this case, the thermal delay in heat flow has increased markedly with the lowered flow rate.

The above shows that thermal transport with gas is significantly more important than the transport via the constantan disk or there would be little change in direction of the major axis of the ellipse or the shape of the ellipse. The TA Instruments recommendation to use helium for experiments with short periods seems well placed and should probably be extended to all periods. The nitrogen results are much further from the in-phase line than the helium results. It is probable that other physical cell designs and material choices could lead to a more responsive system.

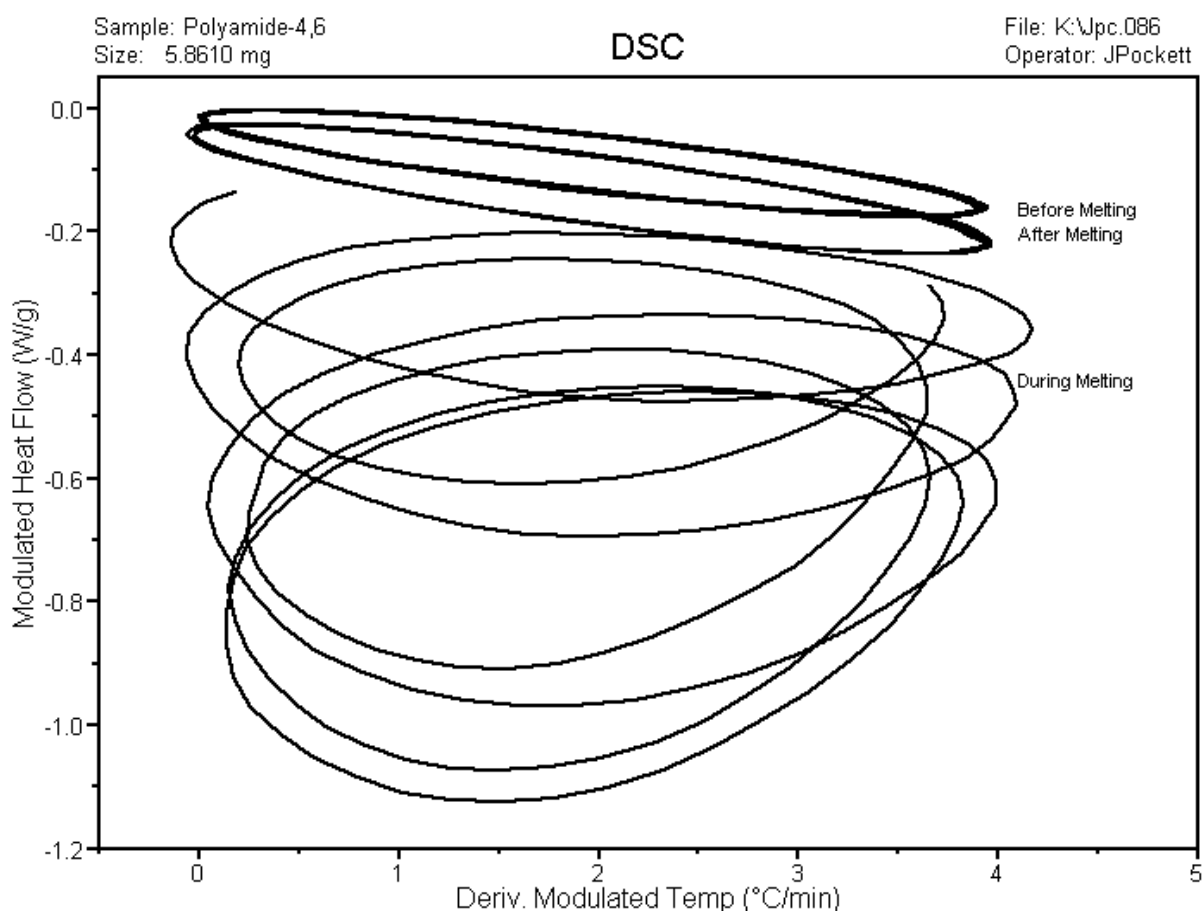


Figure B-6 Lissajous Figure of polyamide-4,6 before, during and after melting in a TMDSC experiment with a 50 ml/min helium purge gas flow, heating rate of 2 0C/min, period of 40 s and an amplitude of 0.212 0C. The three sections are displayed but with portions of the trace leading into and out of the melting removed for clarity. They have not been shifted vertically. CHI_fig6X

A Lissajous plot for polyamide-4,6 before, during and after melting is presented in Figure 6 and demonstrates the distortions to a linear response during melting [162, 177]. The Lissajous loops in Figure B-6 just at the time of going into and out of the melt have been excluded from display for clarity.

The results are typical of other polyamides such as polyamide-6,12, polyamide-6 and polyamide-6,9 measured with TMDSC.

The changing shape of the melting section of the Lissajous Figure B-6 is due to:

- a) The loops descending on the page and then rising again to the post-melt situation. This is due to the average envelope of the heat flow oscillations dipping during the melting. The downward drift of the loops as the polyamide melts are exactly the same as the dip in modulations seen in the inset in Figure B-7. (The perspective in Figure B-7 is a normal one of heat flow versus temperature.)
- b) The height of the oscillations increases markedly. This is due to the increase in heat capacity at the melting temperature. In theory C_p should become infinite just at the melt because of the latent heat of fusion.
- c) The top of the oscillations dips because there is a kinetic component to the melting. There is absorption of energy by kinetic processes at zero heating rates. Much of this is due to the disengagement of macromolecules from lamellae.
- d) The loops become slightly wider at the peak of the melting (the bottom). The heat flow into the sample whilst the reference continues to heat causes an increase in ΔT and this is reflected in the wider range of heating rate because the extra temperature difference must be achieved in the same modulation cycle. That requires a greater heating rate during part of the cycle. The broadening in the temperature derivative direction seen during the polyamide-4,6 melt is similar to that observable in the Lissajous plot in Fig. 8 of Xu *et al.* [171] for crystallisation of amorphous metal alloy.
- e) The loops become rounder indicating phase lags [134]. There are delays built into the melting process. The advantage of studying the

Lissajous figures is that the distortion towards the bottom loop is clearly evident due to large phase changes between the signals

It may be that the “anomalous behaviour” referred to by Cser *et al.* [148] is due to loss of linearity during the melting of HDPE, leading to non-elliptical Lissajous plots rather than the Fourier transformation process.

It can be seen that the top of the Lissajous ellipses do not quite coincide with a zero heat flow even though the rate of heating drops to zero for each modulation. The ellipses are often slightly positive. Dr Mike Reading, the inventor of TMDSC, was queried about this in early 2001. He suspected that the positive heat flow may be due to slight mismatches in pan weights. This does not appear to be the case as in the one experimental run on polyamide-4,6 displayed in Figure B-6 it can clearly be seen that the tops of the ellipses move from the range -0.002 to -0.004 before the melt to the range -0.025 to -0.028 after melting. This is the same run with the same sample and reference pan so that cannot be the case. These differences may possibly be due to baseline curvature.

The amplitude of the modulations has been chosen so that there is zero heating during part of the cycle. That means the Reversing component should be zero at that stage. It would also infer that the “Non-reversing” signal should be touched by the Modulated Heat Flow curves at those points. Figure B-7 shows that this has not occurred and there is a minor deviance of the Non-reversing heat flow signal. It must be noted here that this will only be the case where there is no rapid change in the Non-reversing signal because of the timing effects of the 1½ cycle delay in “temperature” between the instantaneously derived Modulated Heat Flow signal and the computed Non-reversing signal. Further work will be required to clarify this issue which may also be related to the issue above where the top of the Lissajous ellipse, under equilibrium conditions, has a slight negative heat flow rather than zero as expected.

The system has to recover quickly from the perturbation of a melt and that recovery is driven by the block temperature. The sample temperature is utilised as the control element by the instrument, hence there is a feedback response loop involved. A quick response to the perturbations at the sample requires a quick thermal path from the block to the sample pan. This infers

a low thermal resistance that will obviously have some implications with instrument sensitivity. The results will not be valid whilst the system is trying to recover [167].

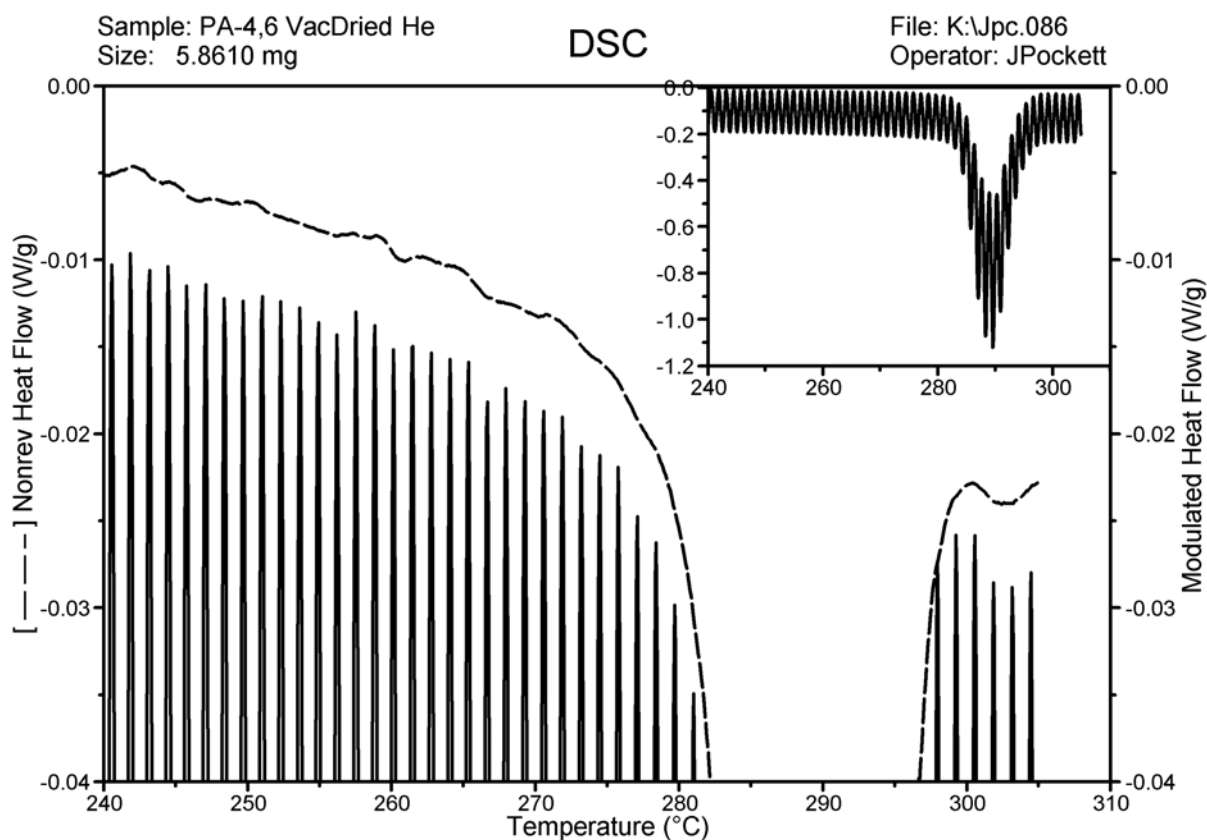


Figure B-7 Non-reversing and Modulated Heat flow versus Temperature for the region around the melting of polyamide-4,6 in TMDSC for a 50 ml/min helium purge gas flow, heating rate of 2 °C/min, period of 40 s and an amplitude of 0.212 °C.

B.4 Conclusions

TMDSC does have the potential to increase sensitivity whilst improving resolution and to separate “Reversible” processes from “Non-Reversible” ones on the time-scale of the experiment.

Heat Capacity (C_p) can be determined on a continuous basis in a relatively quick experiment with TMDSC from a single run on a single small sample and achieve high sensitivity and resolution. The restriction is that accurate heat capacity measurements are most unlikely during major thermal transitions, such as melting and crystallisation.

The method does allow exploration of the effects of in-built stress or ageing on samples, of glass transitions (with some caveats) [180] and of liquid-liquid demixing in polymer-diluent systems [7]. There are limitations as to which transitions can be accurately investigated due to the limitations on TMDSC

of sample size, linearity and the stability of C_p during some thermal transitions.

The results obtained in TMDSC experiments are quite dependent on the experimental conditions but results can easily be monitored by Lissajous plots. The plots of Modulated Heat Flow versus the Derivative of Modulated Temperature can be used to alert to unfavourable experimental conditions where large thermal delays or loss of system linearity can be seen.

TMDSC does require an extra calibration step for accurate determination of heat capacity. Accuracy is extremely important as the results obtained are much more dependent on experimental conditions. Sample preparation is also very important [171].

The choice of purge gas and gas flow rate should aim to approximate the ideal theoretical situation of in-phase signals. In this way transitions can properly be followed in many systems. Helium purge gas is recommended for all TMDSC measurements in TA Instruments Standard Cells because the heat path delays between cell block and the sample and reference pans have been shown to be adversely affected by the use of nitrogen. The flow rate should be at least 50 ml/min. Other types of cells may also require helium purge gas, depending upon their type of construction and the relevant heat flow paths.